Kinetic Energy Budget during Strong Jet Stream Activity over the Eastern United States

HENRY E. FUELBERG

Department of Earth and Atmospheric Sciences, Saint Louis University, Saint Louis, MO 63103

JAMES R. SCOGGINS

Department of Meteorology, Texas A&M University, College Station, TX 77843

(Manuscript received 20 October 1978, in final form 16 October 1979)

ABSTRACT

Kinetic energy budgets are computed during a cold air outbreak in association with strong jet stream activity over the eastern United States. The period is characterized by large generation of kinetic energy due to cross-contour flow. Horizontal export and dissipation of energy to subgrid scales of motion constitute the important energy sinks.

Rawinsonde data at 3 and 6 h intervals during a 36 h period are used in the analysis and reveal that energy fluctuations on a time scale of less than 12 h are generally small even though the overall energy balance does change considerably during the period in conjunction with an upper level trough which moves through the region. An error analysis of the energy budget terms suggests that this major change in the budget is not due to random errors in the input data but is caused by the changing synoptic situation. The study illustrates the need to consider the time and space scales of associated weather phenomena in interpreting energy budgets obtained through use of higher frequency data.

1. Introduction

Kinetic energy budget studies have been performed by various authors on the synoptic (e.g., Chen and Bosart, 1977; Kung, 1977; Sheu and Smith, 1977) and subsynoptic scales (e.g., Kung and Tsui, 1975; Tsui and Kung, 1977) to understand better the complex energy processes that underlie weather events. The present paper presents the kinetic energy budget during an intense cold air outbreak over the eastern United States when a strong jet stream was observed. It differs from studies of similar synoptic situations (e.g., Chen and Bosart, 1977) since a single case is considered in which 3 and 6 h rawinsonde data are used to describe variability often masked by calculations based either on composite cases or longer time intervals between observations. The wintertime period was chosen for this work since most other investigators who used high-frequency observations (e.g., Fuelberg and Scoggins, 1978; Kung and Tsui, 1975; and Tsui and Kung, 1977) considered springtime situations which often coincided with severe storm outbreaks.

2. Kinetic energy equation

The kinetic energy equation given by Smith (1969) is applicable to hydrostatic, open systems. The equation in isobaric coordinates is

$$\frac{\partial K}{\partial t} = \int\int_{\sigma\ p} -\mathbf{V}\cdot\nabla_p\phi - \int\int_{\sigma\ p}\nabla_p\cdot k\mathbf{V} - \int\int_{\sigma\ p}\frac{\partial\omega k}{\partial p} + \int\int_{\sigma\ p}\mathbf{V}\cdot\mathbf{F} + \int_{\sigma} k_0\frac{\partial p_0}{\partial t}, \quad (1)$$

(a) (b) (c) (d) (e) (f)

where

$$\int\int_{\sigma\ p} = \frac{1}{gA}\iiint dxdydp, \quad K = \int\int_{\sigma\ p} k, \quad \phi = gz,$$

and where

- $\mathbf{V}$ horizontal wind vector
- ω vertical motion in isobaric coordinates $[=dp/dt]$
- k horizontal kinetic energy per unit mass $[=(u^2 + v^2)/2]$
- $\mathbf{F}$ frictional force per unit mass
- A area of computation σ.

The subscript zero denotes surface values.

Local changes in kinetic energy for a fixed volume [term (a)] are due to five processes. Term (b) represents kinetic energy generation (Kung, 1966) or conversion of potential to kinetic energy due to cross-contour flow (Smith, 1970). Terms (c) and (d) are horizontal and vertical flux divergences (transports)

0027-0644/80/010069-09$06.25

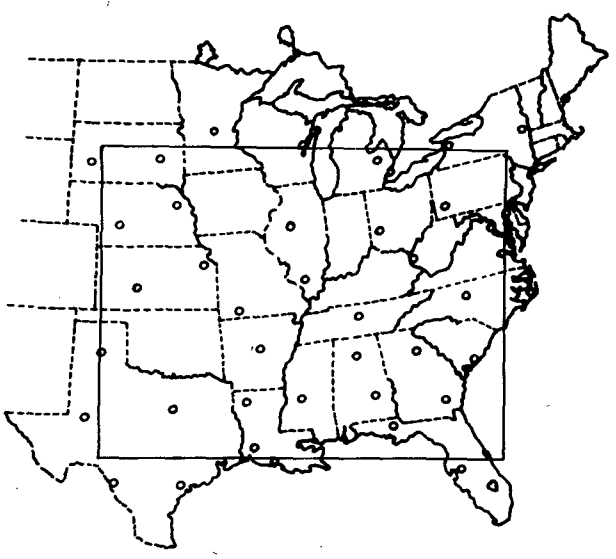

FIG. 1. Locations of rawinsonde stations participating in the AVE III experiment. The budget area is indicated by the solid line.

of kinetic energy, respectively, and represent interaction of the limited volume with the surrounding atmosphere. Term (e) conceptually represents frictional processes, but when computed as a residual in (1), it also represents a transfer of energy between grid and subgrid scales of motion due mostly to unresolvable eddy processes (Smith and Adhikary, 1974). This term is often called the dissipation term and is denoted by D. Term (f) represents changes in kinetic energy due to changes in mass of the volume being studied. Term (f) was found in this study to be at least two orders of magnitude smaller than the remaining terms and will not be considered further.

3. Computational aspects

a. Data

Data from the third Atmospheric Variability Experiment (AVE III) conducted on 6–7 February 1975, and sponsored by the National Aeronautics and Space Administration (NASA), were used in this study. Fig. 1 shows the locations of the rawinsonde stations that participated in the AVE III experiment. Soundings were taken at nine times—at 0000, 0600, 1200, 1500, 1800 and 2100 GMT 6 February, at 0000, 0600 and 1200 GMT 7 February. Procedures used to process the AVE rawinsonde data are described by Fuelberg (1974), and sounding values at 25 mb intervals for the above time periods are provided by Fuelberg and Turner (1975).

Surface observations for 310 stations in the AVE III experiment area, obtained from the National Climatic Center, were used to describe conditions at the surface.

b. Analytical procedures

Since computational procedures for this study were similar to those used by Fuelberg and Scoggins (1978), they will be described only briefly in the present paper. Data were interpolated from the randomly spaced stations onto a grid system with a spacing of 158 km using the Barnes (1964) objective analysis scheme. Gridded analyses of the input data were produced at the surface and at 50 mb intervals from 900 to 100 mb (18 levels). Input wind data were averaged over 50 mb layers to reduce the effects of random errors. Centered finite differences were used where possible to compute all space and time derivatives. However, forward and backward time differences were used for the first and last observation times, respectively.

Grid-point values of terms in (1), except term (e), were computed at each of the 18 levels and integrated over 50 mb layers using the trapezoidal rule. The dissipation term [term (e)] was computed as a residual to balance (1) at each grid point in each 50 mb layer. Kinematic values of vertical motion were used. Terrain-induced vertical motion was included, and an adjustment scheme by O'Brien (1970) was applied so that values at 100 mb equaled those obtained by the adiabatic method.

c. Error analysis

Rawinsonde data are known to possess systematic and random errors (Kurihara, 1961) which can affect values of a derived energy budget. The horizontal and vertical smoothing procedures used in this study (see Fuelberg and Scoggins, 1978) should lessen the affects of such errors, but it is still important to consider how much of the temporal variability of the budget could be due to them. For this purpose, energy budgets were recomputed after random perturbations were added to the original 25 mb values of wind and height data. The procedure is similar to that of Vincent and Chang (1975) and Ward and Smith (1976). Budget values obtained using the perturbed data then were compared to those derived from the original data in order to assess the sensitivity of the various terms. The effects of systematic data errors and computational inadequacies such as truncation error are not considered in this approach.

Computer-generated random perturbations were normally distributed about zero with standard deviations varying as a function of pressure (Table 1). Standard deviations for intermediate levels not given in the Table can be obtained by linear interpolation. These values are similar to those proposed by Kurihara (1961). The 2100 GMT 6 February observation was selected for the sensitivity study because it was the time of maximum kinetic energy content during the period. Ten runs, each with a different

TABLE 1. Standard deviations of normally distributed perturbations.

Pressure level (mb)	Wind direction (deg)	Wind speed (m s^{-1})	Height (m)
100	15.0	5.6	45.5
200	12.7	5.1	37.5
300	10.6	4.5	28.0
500	6.2	3.4	15.0
700	4.0	2.2	10.7
900	2.0	1.1	6.0

set of perturbations at the individual 25 mb levels were made.

Mean absolute differences between the original budget at 2100 GMT and the ten perturbed budgets were computed for three sublayers of the atmosphere and the vertical total (Table 2). Results indicate that the local derivative and dissipation terms are the most sensitive to random errors in the input data. Ward and Smith (1976) noted that the residual dissipation term is unreliable if it occurs as a small difference between two larger terms (the situation at 2100 GMT) but is more reliable if it is of the same order as the primary contributing terms (the situation at some of the remaining times). On the other hand, the terms expressing energy content, generation and horizontal and vertical flux divergence are much more reliable with mean absolute differences usually less than 15% of the original values. The findings of this error analysis generally are similar to those of Chen and Bosart (1977), Vincent and Chang (1975) and Ward and Smith (1976), and will be used in assessing the relative importance of the energy fluctuations described in later sections of this paper.

4. The synoptic situation

The AVE III period was marked by very cold temperatures at the surface and a strong jet stream aloft. Synoptic conditions at the beginning of the experiment, 0000 GMT 6 February 1975, are shown in Fig. 2. A surface frontal system, extending across Georgia through the Florida panhandle and southwestward into the Gulf of Mexico, separated tropical air from polar air. Weak surface cyclones associated with this front were located over Georgia and off the East Coast. A secondary arctic frontal system associated with the low-pressure area over Ohio, extended southwestward along the Appalachians to the Texas Gulf Coast.

A broad trough dominated the upper level flow over the eastern United States and was associated with a closed low over the Hudson Bay region of Canada. The jet stream extended from the Virginia coast southwestward into Texas with a jet maximum with wind speeds as high as 65 m s^{-1} located over the Appalachians.

The weak surface cyclones over Ohio and Georgia moved eastward and offshore during the 36 h period, and by the end of the period, 1200 GMT 7 February, a surface anticyclone was located over eastern Texas (Fig. 3). The circulation around this high dominated the flow at the surface and was bringing arctic air into the eastern half of the country. Southerly flow was producing a warming trend along the western edge of the region.

The trough dominated the upper level flow pattern throughout the period. The trough became sharper as it moved east of the center of the AVE III area. The jet maximum increased to 80 m s^{-1} by the end of the period and moved to a position along the coast of North Carolina.

5. Results

a. Time-averaged budget

The average kinetic energy budget for AVE III was obtained by averaging the kinetic energy budgets for the nine observation times (Table 3). The area of averaging is shown in Fig. 1. The integrated kinetic

TABLE 2. Kinetic energy budget for 2100 GMT 6 February 1975. Values in parentheses are mean absolute differences between the original and ten perturbed budgets. The budget area is shown in Fig. 1.

Pressure layer (mb)	K (10^5 J m^{-2})	$\overline{\partial k/\partial t}$ (W m^{-2})	$\nabla\cdot k\mathbf{V}$ (W m^{-2})	$\overline{\partial \omega k/\partial p}$ (W m^{-2})	$-\mathbf{V}\cdot\nabla\phi$ (W m^{-2})	D (W m^{-2})
400–100	30.2	−0.9	59.8	−8.4	61.0	−10.5
	(0.8)	(6.6)	(4.7)	(1.0)	(6.4)	(10.4)
700–400	14.0	0.6	8.4	8.1	16.2	0.9
	(0.2)	(1.1)	(1.0)	(0.9)	(2.4)	(3.4)
sfc–700	2.9	−1.9	0.3	0.6	6.0	−7.0
	(0.0)	(0.2)	(0.1)	(0.1)	(0.3)	(0.4)
Vertical total	47.1	−2.2	68.5	0.3	83.2	−16.6
	(1.0)	(7.6)	(5.1)	(0.0)	(8.2)	(12.7)

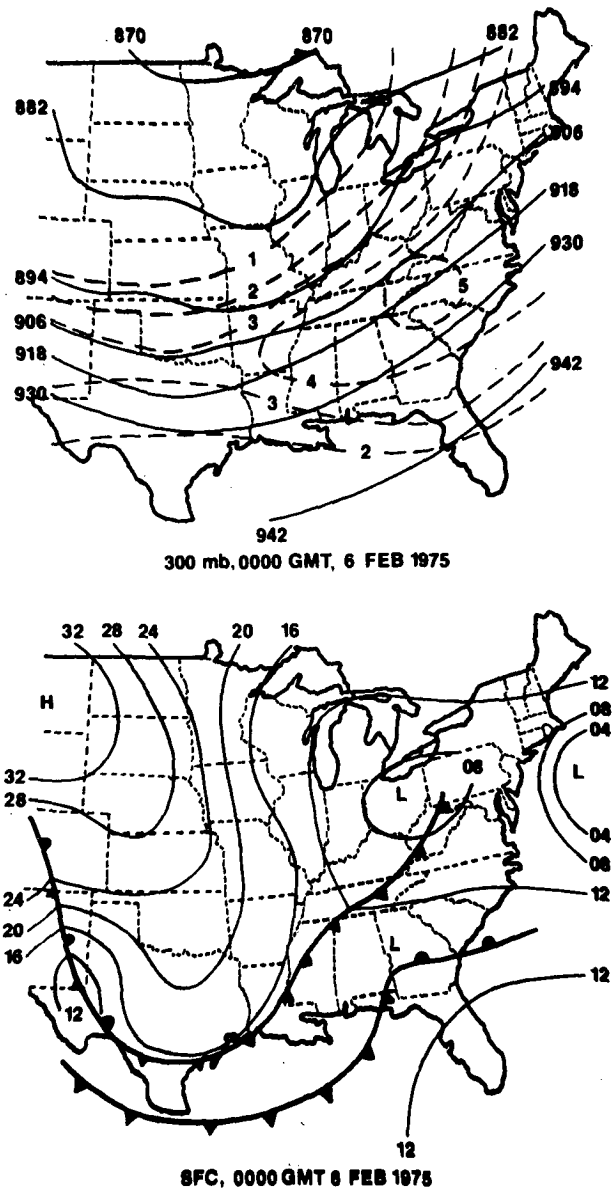

FIG. 2. Synoptic conditions at the beginning of the AVE III experiment, 0000 GMT 6 February 1975. Kinetic energy content of the 400–100 mb layer (10^6 J m^{-2}) is given on the 300 mb map.

energy of the surface to 100 mb layer is 43.2×10^5 J m^{-2}. More than half of this energy occurred above 400 mb in association with the strong jet stream. The local derivative term indicates that average kinetic energy increased slightly with time at all levels during the AVE III period.

Large generation of kinetic energy due to cross-contour flow is the most striking energy process of AVE III. This source of energy is a maximum near the level of the jet stream maximum. A secondary maximum near the surface can be attributed to frictional effects. Large generation of kinetic energy does not result in correspondingly large local increases in kinetic energy because of two additional processes, *viz.*, horizontal transport and dissipation. Large amounts of energy are transported out of the area by horizontal flux divergence, especially near the level of the jet stream maximum (see Table 3), while dissipation acts as a sink of energy at all levels with maxima near the jet and near the surface. Negative values of the dissipation term represent grid-scale to subgrid-scale energy exchanges that are due to viscous frictional loss and eddy dissipation of energy. The magnitude of the vertical transport term is relatively small.

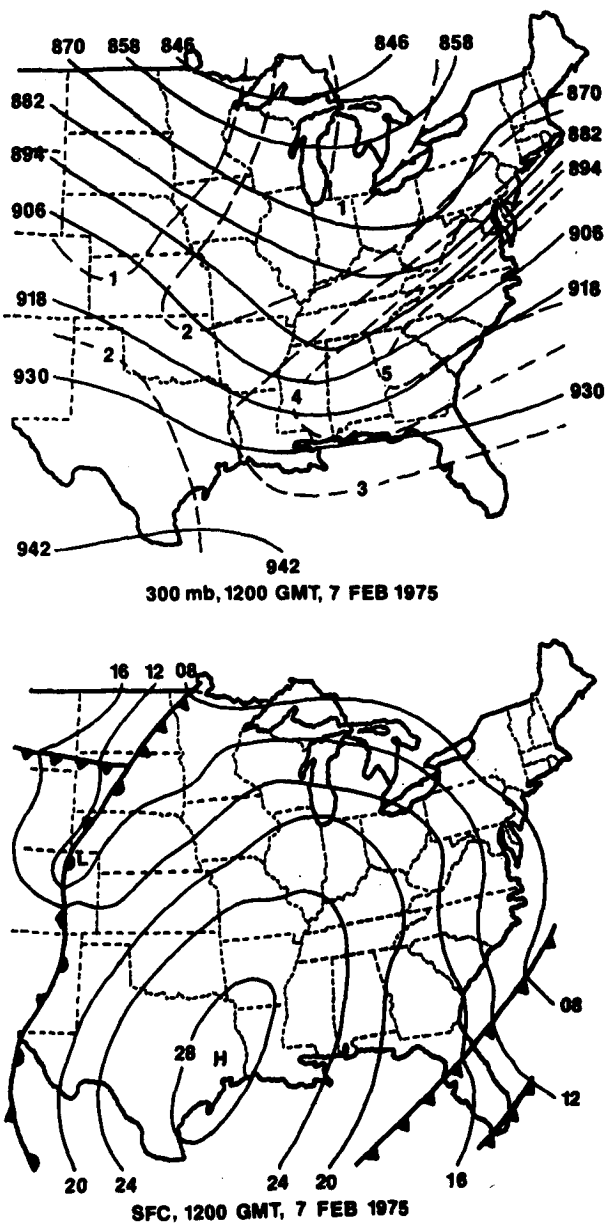

FIG. 3. As in Fig. 2 except at the end of the AVE III experiment, 1200 GMT 7 February 1975.

TABLE 3. Average kinetic energy budget for the entire AVE III experiment. The AVE area is 49.0×10^{11} m^2. All nine observation times are included.

Pressure layer (mb)	K (10^5 J m^{-2})	$\frac{\partial k}{\partial t}$ (W m^{-2})	$\nabla \cdot k\mathbf{V}$ (W m^{-2})	$\frac{\partial \omega k}{\partial p}$ (W m^{-2})	$-\mathbf{V} \cdot \nabla \phi$ (W m^{-2})	D (W m^{-2})
200–100	9.3	0.4	13.0	−0.9	19.3	−6.8
300–200	10.5	1.1	12.6	−0.3	20.1	−6.7
400–300	8.5	1.4	8.2	−0.5	12.6	−3.5
500–400	5.9	0.9	5.3	0.0	7.0	−0.8
600–500	3.9	0.8	2.4	0.4	4.0	−0.4
700–600	2.5	0.3	0.4	0.7	2.2	−0.8
800–700	1.5	0.0	0.2	0.3	1.4	−0.9
900–800	0.8	0.1	0.5	−0.1	1.4	−0.9
sfc–900	0.3	0.0	0.2	−0.1	2.5	−2.4
Vertical total	43.2	5.0	42.8	−0.5	70.5	−23.2
Vertical total using 12 h data only	42.2	3.7	40.9	−0.8	63.2	−19.4

The kinetic energy budget for the AVE III experiment and those of several previous studies are given in Table 4. Attention is called to the fact that various computational procedures were used in these studies.

Few individual case studies using North American data have considered synoptic situations when the jet stream was as intense as observed during AVE III. An exception is the study by Vincent and Chang (1975) who investigated the kinetic energy budget of a North American cyclone during its complete life cycle (Table 4). Magnitudes of several terms of their energy budget are similar to those observed during AVE III, but the signs of some terms, especially the generation term, are opposite to those observed in the present study. The differences are due primarily to differences in the synoptic situations. The locations and movements of jet maxima with respect to the computational areas are major factors in explaining differences in the horizontal flux divergence term. Concerning the generation term, Vincent and Chang noted that the destruction of kinetic energy appearing in their vertical total was due to supergradient flow along the leading edges of troughs in the 500–300 mb layer that occurred in conjunction with the surface cyclone. During AVE III, however, cross-contour flow toward lower heights, causing positive generation, is the dominant process. The large values of generation and transport observed during AVE III and the absence of major cyclone development indicate that strong kinetic energy transformations are not necessarily related to surface developments.

The synoptic-scale environment of the intense squall line studied by Fuelberg and Scoggins (1978) had a lower kinetic energy content than that observed during AVE III, but the magnitudes and signs of the various source and sink terms are comparable (see Table 4). Only the local derivative term differs in sign between the two studies. Winds crossed the contours at rather large angles near the squall line

TABLE 4. The average AVE III kinetic energy budget compared with previous research.

Author	Data	K (10^5 J m^{-2})	$\frac{\partial k}{\partial t}$ (W m^{-2})	$\nabla \cdot k\mathbf{V}$ (W m^{-2})	$\frac{\partial \omega k}{\partial p}$ (W m^{-2})	$-\mathbf{V} \cdot \nabla \Phi$ (W m^{-2})	D (W m^{-2})
Chen and Bosart (1977)**	Cyclone (times 3–5)	—	—	−24.9	−0.4	44.5	−59.1
Vincent and Chang (1975)**	Developing cyclone	47.2	—	50.7*	0.3	−9.2	−27.4
	Mature cyclone	42.3	—	−37.4*	0.2	−0.1	−27.4
Fuelberg and Scoggins (1978)	Squall line synoptic-scale environment	25.4	−6.0	43.9	−0.1	52.2	−14.4
Kung (1977)	AMTEX 1975	66.4	—	25.1	−4.1	50.3	−29.3
Sheu and Smith (1977)	13–16 February AMTEX 1975	63.4	−2.3	53.7	0.0	113.1	−61.7
Present Study	AVE III	43.2	5.0	42.8	−0.5	70.5	−23.2

* Combined boundary flux and system movement.
** Using a moving coordinate system.

TABLE 5. Vertically integrated (surface–100 mb) kinetic energy budget at individual observation times of the AVE III experiment.

Date/time	K (10^5 J m^{-2})	$\frac{\partial k}{\partial t}$ (W m^{-2})	$\nabla \cdot k\mathbf{V}$ (W m^{-2})	$\frac{\partial \omega k}{\partial p}$ (W m^{-2})	$-\mathbf{V} \cdot \nabla \phi$ (W m^{-2})	D (W m^{-2})
6/00	37.1	12.3	36.1	0.2	46.9	1.7
6/06	39.8	12.5	20.3	−0.2	61.5	−28.9
6/12	42.5	12.9	26.7	−2.0	53.1	−15.5
6/15	44.0	19.9	31.6	−1.0	62.2	−11.7
6/18	46.8	14.3	50.7	−1.1	94.7	−30.8
6/21	47.1	−2.2	68.5	0.3	83.2	−16.6
7/00	46.4	−12.6	93.4	−1.1	93.2	−13.5
7/06	43.0	−8.8	40.5	−0.3	80.5	−49.1
7/12	42.6	−1.8	7.2	−0.3	59.7	−54.6

where large values of horizontal velocity divergence and vertical motion were occurring. During AVE III, however, large values of the kinetic energy budget terms resulted more from the strong winds since the crossing angles, velocity divergence and vertical motion were much smaller than in the squall-line case.

Chen and Bosart (1977) did not report values of kinetic energy content in their study of a composite of four cases of polar air penetration into the Caribbean, but some aspects of their synoptic situation are similar to those found during AVE III. Energy budget values for the cyclone accompanying the polar outbreak are given in Table 4. Their values of generation, vertical flux and dissipation are in general agreement with those of the present study; however, strong horizontal flux convergence is indicated in their composite study which is quite the opposite to that observed during AVE III. During the composite study, advection of kinetic energy from an upstream anticyclone into the cyclone region was observed. In AVE III, however, the jet maximum was located on the eastern side of the computational region so that advection of energy out of the region takes place.

Energy budgets for the AMTEX area were similar to those of AVE III, and some similarities in synoptic conditions also are evident. For example, the western Pacific Ocean region, where AMTEX was conducted, is noted for intense jet stream activity. Wind speeds during both a 14-day AMTEX period (Kung, 1977) and a 4-day subperiod encompassing cyclogenesis (Sheu and Smith, 1977) are even stronger than those observed during AVE III. During both AMTEX and AVE III, intense generation of kinetic energy is counteracted by horizontal transport of energy out of the region and dissipation of energy to subgrid scales of motion.

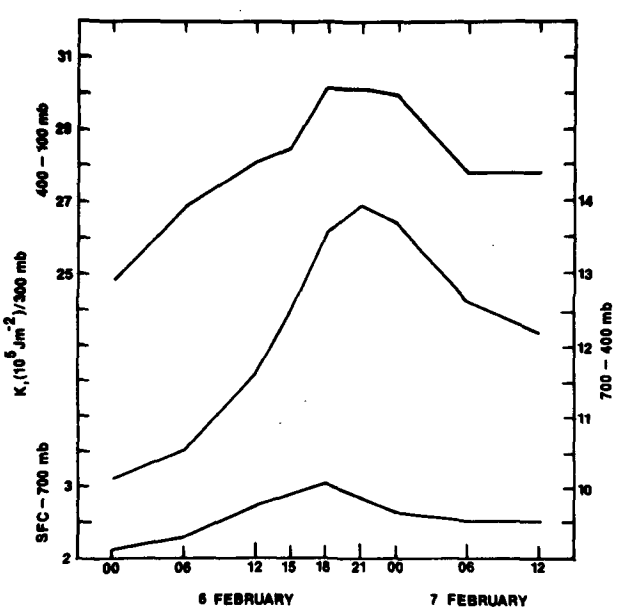

FIG. 4. Time series of kinetic energy content integrated over three sublayers of the atmosphere.

b. Temporal variations

The AVE data permit a rare glimpse into the short-term temporal variability of the kinetic energy budget during the cold air outbreak and associated strong jet stream activity. Vertically integrated budget values at each of the nine observation times are given in Table 5, and integrated values for three sublayers (surface–700 mb, 700–400 mb and 400–100 mb) are given for each time in Figs. 4–8.

The vertical total of kinetic energy content (Table 5) increases from the beginning of AVE III through 2100 GMT 6 February, and then decreases as the region of strongest winds moves out of the AVE area and into the Atlantic Ocean. The vertical total ranges from a low of 37.1×10^5 J m^{-2} to a high of 47.1×10^5 J m^{-2}. Similar relative variations also occurred within the three sublayers (Fig. 4).

Generation of kinetic energy by cross-contour flow roughly follows the changes in kinetic energy content. Table 5 shows that generation for the entire vertical column reaches 94.7 W m^{-2} at 1800 GMT. Fig. 5 reveals that maximum generation in the 400–100 mb layer occurs several hours after the maxima

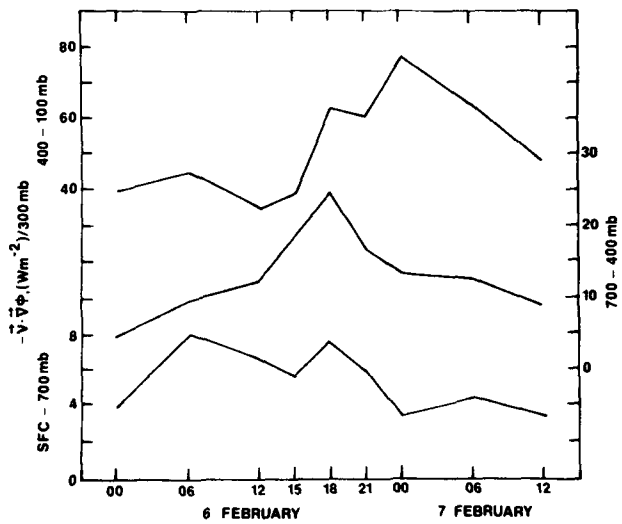

FIG. 5. Time series of generation of kinetic energy integrated over three sublayers of the atmosphere.

in the lower two sublayers due to the tilt of the upper level wave and the extent to which it is encompassed within the budget volume. The values of generation obtained during AVE III are comparable to those reported for synoptic-scale studies of AMTEX 1975 in Table 4 (Kung, 1977; Sheu and Smith, 1977).

Horizontal transport of kinetic energy out of the area occurs in all three sublayers at all nine observation times (Table 5 and Fig. 6). Maximum export in the total column is 93.4 W m^{-2} at 0000 GMT 7 February. By the last observation time, horizontal transport decreases sharply. Export results because stronger winds occur on the eastern side of the network than on the western side.

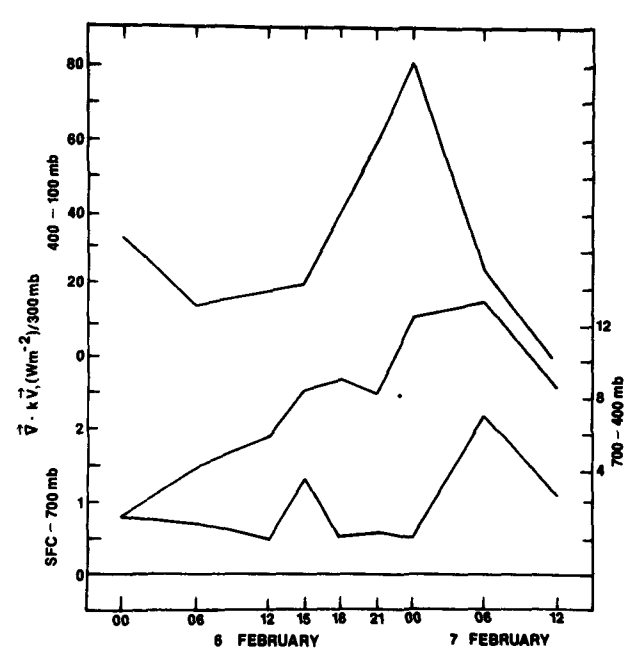

FIG. 6. Time series of horizontal flux divergence of kinetic energy integrated over three sublayers of the atmosphere.

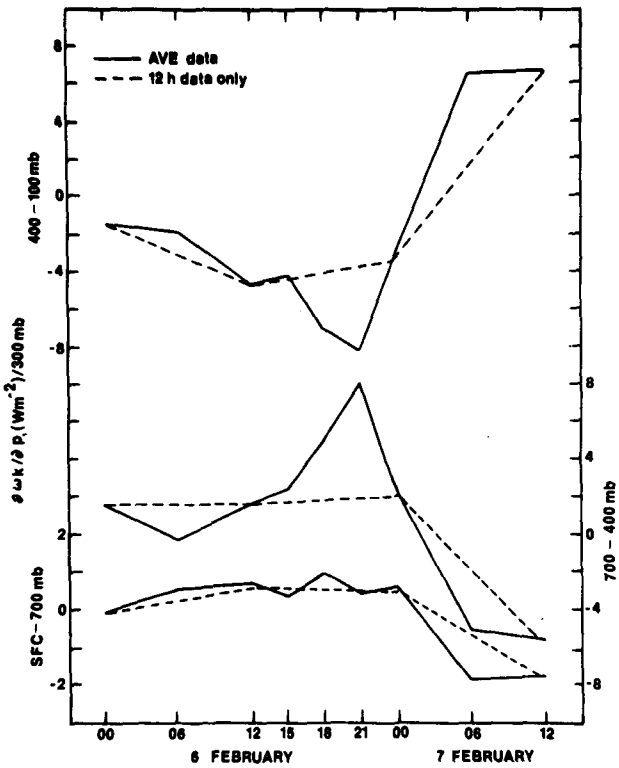

FIG. 7. Time series of vertical flux divergence of kinetic energy integrated over three sublayers of the atmosphere. The solid line indicates values obtained from the 3 and 6 h AVE data while the dashed line indicates the profile that would be obtained with only 12 h data.

Values of vertical transport in the total column are very small due to the boundary limits (Table 5), and are generally smaller than other terms of the budget in individual sublayers, especially the top sublayer (Fig. 7). From the beginning of the period through 0000 GMT 7 February, weak upward vertical motion (<1.0 μb s^{-1} at 500 mb when averaged over the entire area) carries kinetic energy aloft, while during the last two observation times, weak downward vertical motion of about the same magnitude produces the opposite effect. Case studies involving cyclogenesis (e.g., Vincent and Chang, 1975; Chen *et al.*, 1978; Sheu and Smith, 1977; Kung, 1977) have yielded larger values of vertical flux than those observed in AVE III due to their larger areal average vertical motions.

Dissipation of kinetic energy to subgrid scales is an important process during AVE III. Table 5 shows that values of dissipation in the total column range from 1.7 to −54.6 W m^{-2}. Negative dissipation occurs at all but the initial time in the 400–100 mb layer, and at all times in the lowest layer (Fig. 8).

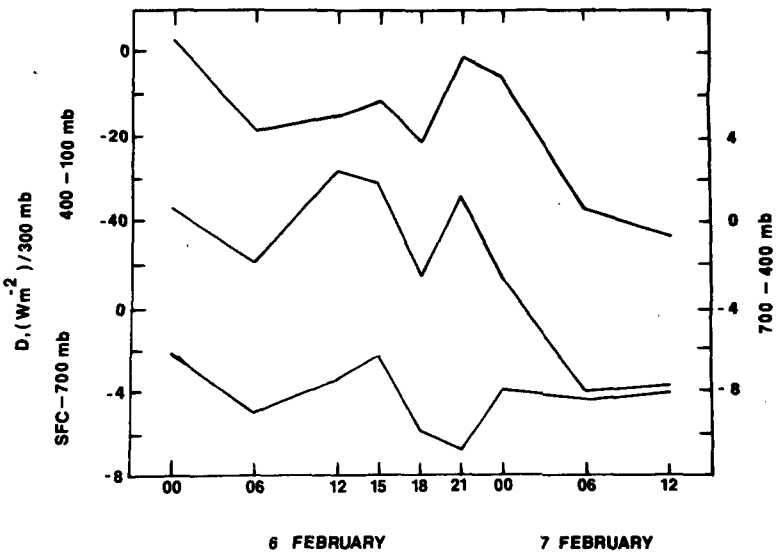

FIG. 8. Time series of dissipation of kinetic energy integrated over three sublayers of the atmosphere.

It is most pronounced during the latter part of the period. Positive dissipation (subgrid processes acting as a source of kinetic energy) is seen in the 700–400 mb layer at some observation times. Since dissipation is calculated as a residual, data and computational uncertainties are factors in producing these positive values. Previous error studies have shown, however, that random errors alone do not account for positive dissipation (Vincent and Chang, 1975; Ward and Smith, 1976). It has been associated with convective activity (Ward and Smith, 1976; Chien and Smith, 1977; Fuelberg and Scoggins, 1978), the damping of upstream turbulence (Ward and Smith, 1976), and interaction with very long waves (Kung and Baker, 1975). During AVE III, turbulence associated with the strong jet may serve as a subgrid-scale energy source to the 700–400 mb layer and as a subgrid-scale sink in the higher levels.

The energy balance undergoes a major change during the course of the AVE III experiment. Horizontal export is the primary energy sink between 0000 GMT 6 February and 0000 GMT 7 February, except for 0600 GMT. Between 33% and 100% of the total generated energy during these times is exported. Dissipative energy losses are of secondary, but not negligible, importance during these same times.

A dramatic change occurs during the last two observation times. Horizontal export decreases significantly in importance while transfer of energy to subgrid scales of motion increases greatly to become the dominant energy sink at the last observation time. These budget changes occur as the surface anticyclone becomes centered over the area and the upper level trough and region of strongest winds move eastward to be replaced by more zonal conditions and warmer temperatures.

The fluctuations in kinetic energy balance during AVE III are generally consistent with those observed during AMTEX 1975 by Kung (1977) i.e., kinetic energy content and cross-contour generation of kinetic energy increased during cold air outbreaks and decreased during warm periods.

Results of the present study suggest that the major energy changes during this particular period are resolved fairly well by 12 h data when the observation times of 0000 and 1200 GMT are chosen. Fig. 7 shows the fluctuations that would have been undetected in the vertical flux term with 12 h data alone (dashed line). Figs. 4–8 indicate that many of the budget terms were either at or near maximum or minimum values for the 36 h period near 0000 GMT 7 February. Some other choice of the 12 h interval would have resulted in a less accurate description of the energy variability during AVE III. For most terms of the budget (Figs. 4–8, Table 5) the magnitudes of the fluctuations with periods less than 12 h are comparable to those resulting from the introduction of random errors (Table 2). Therefore, to further investigate the usefulness of the 3 h data during this particular period, an energy budget for the entire experiment area and period was computed using only standard rawinsonde data at 0000 and 1200 GMT. The local derivative term also was computed based on the 12 h data alone. Results for the surface to 100 mb layer are given at the bottom of Table 3. The energy balance based on nine observation times is very similar to that obtained from only four observations at 12 h intervals.

The results just described for AVE III contrast

with those found during AVE IV, a springtime severe storm situation, when important fluctuations in the synoptic-scale energy balance were observed (Fuelberg and Scoggins (1978)). Likewise, the energy balance of mesoscale storm environments was found to be highly variable by Kung and Tsui (1975) and Tsui and Kung (1977) who used NSSL data at 1.5 h intervals. Apparently, no other energy studies of winter situations have been made using 3 h rawinsonde data, but such data sets and studies derived therefrom would be valuable in describing variations in the atmospheric energy cycle.

6. Summary

A kinetic energy budget has been presented for the eastern United States during a cold air outbreak in association with strong jet stream activity. Rawinsonde data at 3 or 6 h intervals are used to describe energy processes during the outbreak. Most previous energy studies based on higher frequency data have considered springtime severe storm situations, not wintertime periods.

Large generation of kinetic energy by cross-contour flow, horizontal export of energy, and transfer of energy from grid to subgrid scales of motion are the primary features of the kinetic energy budget. The energy balance during the initial times of the AVE III period changes considerably by the last observation time as a long-wave trough moves through the region.

In contrast to the severe storm situations studied using higher frequency data, significant energy variability with periods less than 12 h is not observed during AVE III on the space scale of the data used. The study is representative of a situation when the major weather events are occurring on the synoptic scale. It quantitatively points out intuitively conceived relationships between high-frequency energy fluctuations and subsynoptic-scale weather occurrences and serves to caution against the generalized interpretation of case studies without a companion analysis of the time and space scales of associated weather phenomena.

While error analyses indicate that the dissipation term is the most suspect to random errors in the input data, values of other major contributing terms are more reliable. Long-term trends of all terms appear meaningful.

Acknowledgments. Sincere appreciation is expressed to Dr. Donald E. Martin for reading the manuscript and for offering many helpful suggestions. Special thanks are due Cathy Nicksich for typing the manuscript and Bill Abeling and David Ebel for preparing the figures. The comments of the reviewers who made excellent suggestions for improving and clarifying the article are sincerely appreciated.

This research was sponsored by the National Aeronautics and Space Administration under Contract NAS8-31773 to Texas A&M University and Contract NAS8-32838 to Saint Louis University. Both contracts were under the auspices of the Aerospace Environment Division, Space Sciences Laboratory, NASA Marshall Space Flight Center, Alabama.

REFERENCES

Barnes, S. L., 1964: A technique for maximizing detail in numerical weather map analysis. *J. Appl. Meteor.*, **3**, 396–409.

Chen, T. C., J. C. Alpert and T. W. Schlatter, 1978: The effects of divergent and nondivergent winds on the kinetic energy budget of a mid-latitude cyclone: A case study. *Mon. Wea. Rev.*, **106**, 458–468.

Chen, T. J., and L. F. Bosart, 1977: Quasi-Lagrangian kinetic energy budgets of composite cyclone-anticyclone couplets. *J. Atmos. Sci.*, **34**, 452–464.

Chien, H., and P. J. Smith, 1977: Synoptic and kinetic energy analyses of Hurricane Camille (1969) during transit across the southeastern United States. *Mon. Wea. Rev.*, **105**, 67–77.

Fuelberg, H. E., 1974: Reduction and error analysis of the AVE II pilot experiment data. NASA CR-120496, George C. Marshall Space Flight Center, Alabama, 131 pp.*

——, and R. E. Turner, 1975: Data for NASA's AVE III experiment: 25-mb sounding data and synoptic charts. NASA TM X-64938, George C. Marshall Space Flight Center, Alabama, 462 pp.*

——, and J. R. Scoggins, 1978: Kinetic energy budgets during the life cycle of intense convective activity. *Mon. Wea. Rev.*, **106**, 637–653.

Kung, E. C., 1966: Kinetic energy generation and dissipation in the large-scale atmospheric circulation. *Mon. Wea. Rev.*, **94**, 67–82.

——, 1977: Large-scale energy transformations in the intense winter monsoon over the Kuroshio region. *J. Meteor. Soc. Japan*, **55**, 498–510.

——, and W. E. Baker, 1975: Energy transformation in middle latitude disturbance. *Quart. J. Roy. Meteor. Soc.*, **101**, 793–815.

——, and T. L. Tsui, 1975: Subsynoptic-scale kinetic energy balance in the storm area. *J. Atmos. Sci.*, **32**, 729–740.

Kurihara, Y., 1961: Accuracy of winds aloft data and estimation of errors in numerical analysis of atmospheric motions. *J. Meteor. Soc. Japan*, **39**, 331–345.

O'Brien, J. J., 1970: Alternate solution to the classical vertical velocity problem. *J. Appl. Meteor.*, **9**, 197–203.

Sheu, Y. T., and P. J. Smith, 1977: Kinetic energy budget analyses during a subperiod of the Air Mass Transformation Experiment 1975. *Mon. Wea. Rev.*, **105**, 1501–1507.

Smith, P. J., 1969: On the contribution of a limited region to the global energy budget. *Tellus*, **21**, 202–207.

——, 1970: A note on energy conversions in open atmospheric systems. *J. Atmos. Sci.*, **27**, 518–521.

——, and S. P. Adhikary, 1974: The dissipation of kinetic energy in large-scale atmospheric circulations. *Rev. Geophys. Space Phys.*, **12**, 281–284.

Tsui, T. L., and E. C. Kung, 1977: Subsynoptic-scale energy transformations in various severe storm situations. *J. Atmos. Sci.*, **34**, 98–110.

Vincent, D. G., and L. N. Chang, 1975: Kinetic energy budgets of moving systems: Case studies for an extratropical cyclone and hurricane Celia, 1970. *Tellus*, **27**, 215–233.

Ward, J. H., and P. J. Smith, 1976: A kinetic energy budget over North America during a period of short synoptic wave development. *Mon. Wea. Rev.*, **104**, 836–848.

* Available from Space Sciences Laboratory, NASA/Marshall Space Flight Center, Alabama.